Solution Conformation of Human Apolipoprotein C-1 Inferred from Proline Mutagenesis: Far- and Near-UV CD Study†

Olga Gursky*

Department of Physiology and Biophysics, Boston University School of Medicine, 715 Albany Street, Boston, Massachusetts 02118

Received June 4, 2001; Revised Manuscript Received July 23, 2001

ABSTRACT: Solution structure of lipid-free apolipoprotein C-1 (apoC-1, 6.6 kD) was analyzed by circular dichroism (CD) of 15 mutants containing single Pro or Ala substitutions in predicted α-helical regions. While the majority of Pro substitutions induce complete (L11P, L18P, R23P, I29P, M38P, W41P, T45P) or partial (G15P, L34P) helical unfolding, similar substitutions at other sites (A7P, Q31P, V49P, L53P) do not cause large changes in the secondary structure or stability. The results suggest that lipid-free apoC-1 is comprised of two dynamic helices that are stabilized by interhelical interactions and are connected by a short linker containing residues 30−33. We propose that the minimal folding unit in the lipid-free state of this and other exchangeable apolipoproteins comprises the helix−turn−helix motif formed of four 11-mer sequence repeats. Comparison of the helical content in lipid-free and lipid-bound apoC-1 suggests that lipid binding shifts the conformational equilibrium toward preexisting highly helical conformation. Remarkably, near-UV CD spectra of wild type and mutant apoC-1 are not significantly altered upon thermal or chemical unfolding and thus result from residual aromatic clustering that is retained in the unfolded state. Correlation of far- and near-UV CD of the mutant peptides suggests that the hydrophobic cluster containing W41 is essential for the helical stability and may form a helix nucleation site in apoC-1.

Lipids in the body are transported in the form of lipoproteins that are macromolecular complexes of varying lipid and protein composition, size, density, and metabolic properties (*1*−*3*). For example, high-density lipoproteins (HDL)[1] mediate cholesterol removal from peripheral tissue, low-density lipoproteins (LDL) mediate cholesterol delivery, and the balance between HDL and LDL correlates with the probability of developing atherosclerosis (*1*−*3*). Exchangeable apolipoproteins are water-soluble protein components of lipoproteins that solubilize lipids and regulate their metabolism by binding to cell receptors or activating specific enzymes such as lecithin:cholesterol acyltransferase (LCAT) whose reaction is key in reverse cholesterol transport (*4*). Human apolipoprotein C-1 (apoC-1, 57 a.a.) is the smallest exchangeable apolipoprotein. ApoC-1 transfers among HDL ($d \sim 100$ Å), very low-density lipoproteins (VLDL, $d \sim 600$ Å) and chylomicrons ($d \sim 2000$ Å) (*1*, *5*). On HDL, apoC-1 is a potent activator of LCAT (*6*, *7*) and a major inhibitor of cholesteryl ester transfer protein that promotes the exchange of neutral lipids between HDL and LDL (*8*). ApoC-1 can also inhibit hepatic lipase (*9*) and phospholipase A2 (*10*) and can stimulate cell growth (*11*). In addition, apoC-1 delays the clearance of potentially atherogenic β-VLDL by inhibiting their uptake via the apoE-mediated LDL receptor-related pathway (*12*−*14*). Even though the apoC-1 functions are carried out on lipoproteins, nascent apoCs are secreted predominantly in their lipid-poor forms (*14*). The conformation of lipid-poor or lipid-free apoC-1 is also proposed to control apoC-1 transfer among lipoproteins (*15*). Thus, in the course of its metabolism, apoC-1 adapts its conformation to various lipoproteins and to the lipid-poor state in plasma. This structural adaptability is a distinct property of the exchangeable apolipoproteins that is essential for their function and plasma transfer and is attributed to refolding and repacking of the constituent α-helices.

The amino acid sequences of the exchangeable apolipoproteins contain 11/22-mer tandem repeats forming distinct amphipathic α-helices (*16*). Class-A α-helices, that are predominant in apolipoproteins, differ from those found in globular or membrane proteins by their large (30−50%) apolar surface area that is involved in lipid binding and by characteristic distribution of charged groups (*16*). ApoC-1 contains four such 11-mer repeats encompassing residues 7−50, and is predicted to form two class-A α-helices, 7−32 and 33−53 (*17*) that are important for the lipid binding (*18*−*20*). High sequence homology (11-mer tandem repeats), structural (class-A α-helices) and functional similarity of apoC-1 and larger apolipoproteins (LCAT activation, forma-

† This work was supported by the National Institute of Health Grant HL61429. CD instrument was supported by the NIH Grant HL26335 (D. M. Small, P. I.)

* Phone: (617) 638-7894. FAX: (617) 638−4041. E-mail: Gursky@med-biophd.bu.edu.

[1] Abbreviations: Apo, apolipoprotein; WT, wild type; HDL, high-density lipoprotein; LDL, low-density lipoprotein; VLDL, very low-density lipoprotein; β-VLDL, β-migrating very low-density lipoprotein; LCAT, lecithin:cholesterol acyltransferase; TMAO, trimethylamine-*N*-oxide dihydrate; Gdn Cl, guanidinum hydrochloride; UV CD, ultraviolet circular dichroism; NMR, nuclear magnetic resonance; SDS, sodium dodecyl sulfate.

10.1021/bi0111505 CCC: $20.00
Published on Web 09/15/2001

tion of discoidal complexes with phospholipids, displacement of apoE from β-VLDL) make apoC-1 an attractive model system for the analysis of the structural stability and adaptability in relation to apolipoprotein functions.

In their lipid-free state in solution, apoC-1 and other exchangeable apolipoproteins have structural (compact shape, substantial α-helical content, lax tertiary packing) and thermodynamic properties (low stability $\Delta G(25\ ^\circ C) < 2.5$ kcal/mol, broad heat unfolding transition, etc.) consistent with the molten globular state (*21*, *22*). Lipid binding is accompanied by helical rearrangement and by an increase in the α-helical content. The largest increase is observed in apoC-1, from an average of 31% α-helix in the lipid-free monomer in solution (*22*) up to 75% in lipid-bound or self-associated states (*15*, *23*). The molecular mechanism of this transition is unclear, whereas the mechanisms of functional transitions in other human apolipoproteins are beginning to be elucidated (*24*, *25*). Specifically, it is unclear whether lipid binding induces folding of additional helical segments in apoC-1 (which would be the case if ~30% of apoC-1 groups formed α-helices in solution) or shifts the conformational equilibrium toward a preexisting highly helical conformation (which would be the case if the monomer was highly helical ~1/3 of time).

The aim of this work is to determine the structure of lipid-free apoC-1 monomer in solution and compare it with the NMR structure of apoC-1 on "lipid-mimicking" SDS micelles (*20*). Solution NMR cannot be used for solving the structure of lipid-free apoC-1 monomer because of the protein self-association at >0.01 mg/mL concentrations (*15*). In contrast, far-UV CD that utilizes 0.01−0.1 mg/mL protein solutions is suitable for the structural analysis of lipid-free apoC-1 monomer (*22*) but does not provide secondary structure assignment to individual groups. To make such an assignment, we use far-UV CD in conjunction with proline scanning mutagenesis. Our approach is based upon observation that Pro is known to destabilize protein α-helices by introducing steric strain, leaving the unsaturated H-bond of (i-4) backbone carbonyl and preventing H-bond formation between the (i-3) carbonyl and the (i+1) amide. The destabilizing effect of Pro substitutions in the middle of the α-helices in globular proteins, $\delta\Delta G = -2.7$ to -5.6 kcal/mol (*26* and references therein), is larger than the apoC-1 monomer stability, $\Delta G(25\ ^\circ C) = 1.8$ kcal/mol (*22*). Therefore, single Pro substitutions in the α-helical region(s) should substantially unfold the apoC-1 molecule. In contrast, Pro substitutions in disordered or loop regions should cause no destabilization or unfolding (*27*, *28*). Utilization of this approach in our earlier far-UV CD study showed that Pro substitutions at different sites have contrasting effects on the apoC-1 conformation: L11P, R23P, and T45P induce complete helical unfolding, G15P causes partial unfolding, and Q31P leads to no unfolding/destabilization (*29*). In the current work, we combine these results with far-UV CD analyses of eight additional Pro-containing mutants to propose a model structure of lipid-free apoC-1 monomer in solution. We also report the first near-UV CD study of apoC-1 and 15 Pro- or Ala-containing mutants that is facilitated by the presence of one Trp (W41) and three Phe (F14, F42, F46) in the apoC-1 sequence. To our knowledge, this is the first observation of a near-UV CD from the thermally, chemically, and Pro-unfolded protein states.

EXPERIMENTAL PROCEDURES

Peptides. Human wild type (WT) and mutant apoC-1 containing single Pro substitutions in the predicted α-helices 7−32 and 33−53 were used, including five mutants reported earlier (L11P, G15P, R23P, Q31P, and T45P) and eight additional mutants (A7P, L18P, I29P, L34P, M38P, W41P, V49P, and L53P). Proline substitutions were introduced, one at a time, at apolar sites with an average separation of 3−4 groups, i.e., about one helical turn. The peptides were obtained by solid state synthesis as described (*29*) utilizing the published protocols (*30*, *31*); the peptide N- and C-termini were not chemically blocked. The peptides were purified by HPLC to 95−98% purity that was assessed by mass spectroscopy and SDS gel electrophoresis. Lyophilized peptides were dissolved in 4 mM sodium phosphate buffer (pH 7.6−7.8) to 1−2 mg/mL concentration and diluted by buffer or buffer/osmolyte solution (pH 7.8) for CD experiments. Wild-type human apoC-1 monomer prepared by this method was demonstrated to have secondary structure and thermodynamic parameters similar to those of the plasma protein (*29*). Peptide concentration was assessed by UV absorption at 280 nm and by chromatographic Lowry assay. All chemicals were the highest purity analytical grade.

Far- and Near-UV CD Measurements. CD spectroscopic data were recorded with an AVIV 62-DS spectrophotometer equipped with Peletier temperature control and calibrated with camphorosulfonic acid. The CD monochromator upgrade, that included installation of mirrors with optimized far-UV reflectivity, substantially improved signal-to-noise ratio in far- and near-UV, thereby facilitating the first near-UV CD analysis of apoC-1. Far-UV CD spectra (185−250 nm) and the thermal unfolding curves were recorded from protein solutions of 0.007−0.01 mg/mL concentrations placed in 2−10 mm quartz cuvettes. Since at ≤ 0.01 mg/mL concentrations and the buffer conditions used in our far-UV CD experiments human WT apoC-1 is fully monomeric (*15*, *29*), mutant peptides containing Pro substitutions of apolar groups are also expected to be monomeric. Near-UV CD spectra (250−330 nm) were recorded from protein solutions of 0.07−1.0 mg/mL concentrations placed in 5−10 mm quartz cuvettes. Near-UV CD spectrum of V49P apoC-1, that has relatively high intensity, was also recorded from protein solution of 0.03 mg/mL concentration at which apoC-1 is expected to be partially monomeric (*15*). Near-UV CD spectra of all peptides were also recorded in the presence of 1.2 M Gdn HCl where apoC-1 is monomeric and its secondary structure is unfolded (*20*). The spectra were recorded with 1-nm bandwidth, 0.5−1 nm increment, and 15 s accumulation time, and averaged over 2−5 scans. Thermal unfolding curves were recorded at 222 nm or other characteristic wavelengths upon heating from 5 to 95 °C at a rate of 30−90 °C/h, with a 0.5−2 °C increment, 60−99 s accumulation time. The melting curves recorded at different heating rates fully superimposed, and the spectra recorded at 20 °C before and after a brief heating to 70 °C overlapped, confirming the reversibility of the transition. Following the buffer baseline subtraction, the CD data were normalized on protein concentration, smoothed by a third degree polynomial, and are reported as molar residue ellipticity, [Θ]. Peptide α-helical content was estimated from the molar residue ellipticity at 222 nm, [Θ_{222}] (*32*), and by far-UV CD

spectral deconvolution using software package ProtCD (*33*) (courtesy of Dr. S. Venyaminov); these estimates agreed within 5% accuracy. The melting temperature T_m and effective enthalpy $\Delta H_v(T_m)$ were determined by conventional van't Hoff analysis of the $[\Theta_{222}](T)$ data and confirmed by fitting the data and the baselines to an extended form of van't Hoff equation (*29* and references therein); T_m and $\Delta H_v(T_m)$ were also estimated from the differential melting curves $d[\Theta_{222}]/dT$ (*34*). Two latter approaches are particularly useful for the analysis of broad transitions, such as apoC-1 unfolding, that lack well-defined pre- and/or post-transitional baselines. ORIGIN software (Microcal, Inc.) was used for the CD data analysis and display.

RESULTS

Far-UV CD of Pro-Containing apoC-1 Mutants. Far-UV CD data recorded of selected Pro-containing mutants are shown in Figure 1. These data fall into three groups; the largest group includes the closely superimposable spectra of L11P, L18P, R23P, I29P, M38P, W41P, and T45P (Figure 1A, open circles). These spectra do not change significantly over the temperature range analyzed (5−90 °C), as illustrated by the difference spectra recorded at 20 and 90 °C (Figure 1A, inset) and by the nearly constant ellipticity $[\Theta_{222}](T)$ observed at 5−90 °C (Figure 1B, open circles). CD spectral deconvolution indicates that the α-helical content in these peptides does not exceed 5−10%, with the random coil content approaching 90%. Thus, Pro substitutions in these peptides induce complete helical unfolding. The second group includes G15P and L34P whose far-UV CD data (Figure 1A, triangles) suggest an incompletely folded state, as indicated by the α-helical content of 20% for G15P (*29*) and 15% for L34P at 20 °C (as compared to 31% for WT), by the difference spectra between 20 and 90 °C showing the loss of the helical structure upon heating (Figure 1A, inset) and by the temperature dependence of $[\Theta_{222}]$ (Figure 1B, triangles). The third group comprises Q31P (Figure 1A, solid circles), A7P, V49P, and L53P mutants that show no large changes in their far-UV CD spectra or thermal unfolding data as compared to the WT (Figure 1A, solid line). The melting temperature $T_{m,Q31P} = 51 \pm 1.5$ °C and effective enthalpy $\Delta H_{v,Q31P}(T_m) = 19 \pm 2$ kcal/mol of Q31P determined from the analysis of its thermal unfolding data (Figure 1B, solid circles) are similar to those of the WT ($T_{m,WT} = 50 \pm 2$ °C, $\Delta H_{v,WT}(T_m) = 18 \pm 2$ kcal/mol, (*29*)), suggesting similar apparent free energy of stability $\Delta G_{app}(25\ °C) \sim 1.8$ kcal/mol. Similar values of T_m and $\Delta H_v(T_m)$ were obtained for A7P, V49P, and L53P. In summary, A7P, Q31P, V49P, and L53P substitutions do not cause large changes in the apoC-1 secondary structure or stability.

Near-UV CD of Wild Type and Mutant apoC-1. Near-UV CD spectra of WT (Figure 2) were recorded over a broad range of protein concentrations, temperatures, and osmolyte concentrations and were correlated with the secondary and/or quaternary structural changes observed in apoC-1 under these conditions (*15*, *29*). In buffer solution at 0.2 mg/mL protein concentration, near-UV CD of the WT (Figure 2, solid line) is dominated by the contribution from W41, with the positive peak centered at 295 nm and a shoulder at 285 nm corresponding to vibronic components of ^1L_b transition in Trp (*35*). The spectral amplitude at 295 nm corresponds to molar ellipticity of 6 800 deg cm^2 dmol^{-1} per Trp, or to molar CD of $\Delta\epsilon = 2.05$ M^{-1} cm^{-1}, consistent with the value expected for constrained Trp (*35*). A smaller negative peak centered at 263 nm corresponds to ^1L_b transition of Phe arising from contributions of F14, F42, and/or F46; this peak may also contain background contribution from the broad ^1L_a band of Trp centered at 270 nm (*35*, *36* and references therein).

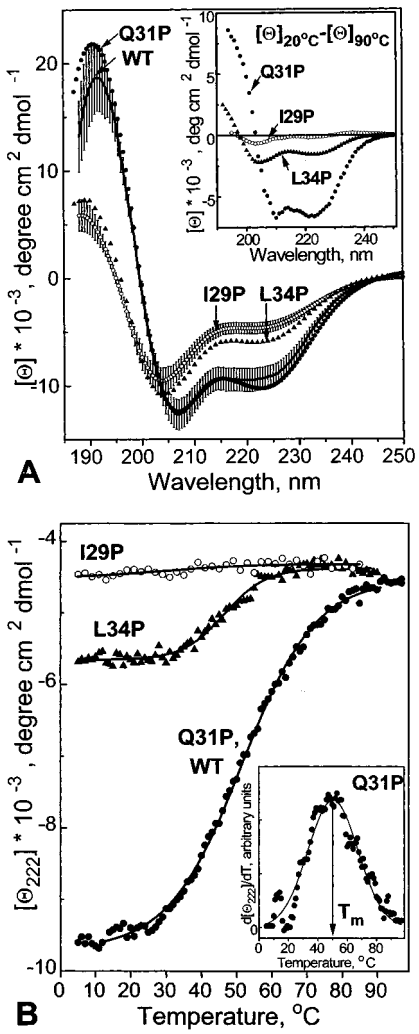

FIGURE 1: Far-UV CD data of apoC-1 containing single Pro substitutions at selected sites. (A) The spectra recorded from 0.01 mg/mL peptide solutions in 4 mM sodium phosphate buffer, pH 7.6, at 20 °C: WT (—), shaded area shows the range for the overlapping spectra of A7P, V49P, L53P, and Q31P (●); L34P (▲); I29P (○); shaded area shows the range for closely overlapping spectra of L11P, L18P, R23P, M38P, and T45P. Inset: Difference spectra $[\Theta]_{20°C} - [\Theta]_{90°C}$ between the data recorded at 20 and 90 °C. (B) Thermal unfolding of apoC-1 peptides monitored at 222 nm upon heating the peptide solutions from 5 to 95 °C. Line coding as in panel A; solid lines show data fitting by a sigmoidal function. For Q31P, this sigmoidal function coincides with the data fitting by an expanded van't Hoff equation (*29* and references therein). The melting data and the van't Hoff plot of Q31P closely superimpose those of the WT monomer (*29*). For L34P, reduced amplitude of $[\Theta_{222}]$ leads to low signal-to-noise ratio that precludes accurate van't Hoff analysis. Inset: first derivative $d[\Theta_{222}]/dT$ for Q31P. Arrow shows the peak center corresponding to the melting temperature $T_m = 51 \pm 1.5$ °C of Q31P that is similar to $T_m = 50 \pm 2$ °C of the WT (*29*).

Importantly, near-UV CD of WT is invariant over the protein concentration range analyzed (0.07−1 mg/mL), indicating that the changes in the degree of apoC-1 oligomerization that occur at these concentrations and buffer

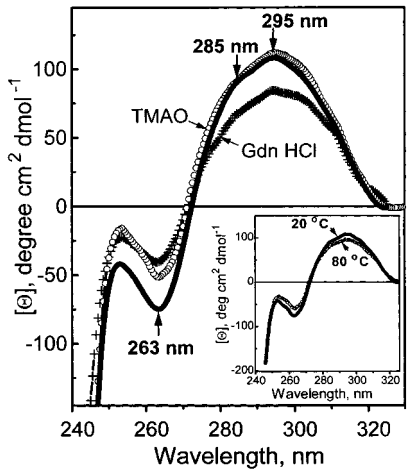

FIGURE 2: Near-UV CD spectra of WT apoC-1 under various environmental conditions. The data were recorded at 20 °C, pH 7.8, from 0.2 mg/mL protein solutions containing 4 mM sodium phosphate buffer (—); 4 mM buffer + 1.4 M Gdn HCl (+); 4 mM buffer + 1.4 M TMAO (○); identical near-UV CD were obtained from peptide solutions of 0.07−1 mg/mL concentrations. The bands of Trp (L_B at 295 and 285 nm) and Phe (at 263 nm) are indicated. Inset: Spectra of 0.2 mg/mL WT solution in 4 mM buffer at 20 °C (—) and at 80 °C (◇).

conditions (*15*) do not significantly alter the packing of the aromatic groups. Remarkably, comparison of the near-UV CD spectra recorded at 20 °C from 0.07 to 1 mg/mL apoC-1 in the absence and in the presence of 1.4 M Gdn HCl (Figure 2, solid and crossed lines compared) shows that apoC-1 dissociation into monomers followed by the chemical unfolding of the monomer α-helical structure that occurs between 0 and 1.2 M Gdn HCl (*22*) has no large effect on the near-UV CD. Similarly, near-UV CD of WT at any concentration used (0.07−1 mg/mL) is almost invariant in the temperature range analyzed (5−95 °C): the spectra recorded from the same sample at 20 and 80 °C largely overlap (Figure 2, inset), and the ellipticity at 295 nm is nearly invariant upon heating from 5 to 95 °C (data not shown). Consequently, thermal unfolding of the α-helical structure in apoC-1 that occurs upon heating from 25 to 80 °C (*22*, *29*) does not significantly alter the packing of the aromatic residues. Furthermore, the overlapping spectra recorded at 25 °C in the presence of 0−1.4 M trimethylamine-*N*-oxide (TMAO) (Figure 2, solid line and open circles compared) show that the previously demonstrated TMAO-induced apoC-1-folding, with an increase in the α-helical content from 31 to 75% observed upon increasing TMAO concentration from 0 to 1.4 M (*29*), has no large effect on the near-UV CD. In summary, the data in Figure 2 demonstrate that large secondary and/or quaternary structural changes in WT apoC-1, from <5% α-helix (in the monomeric state in 1.4 M Gdn HCl, or at >80 °C) to 75% α-helix (in self-associated state in 1.4 M TMAO), have little effect on its near-UV CD.

Near-UV CD spectra of Pro-containing apoC-1 mutants are displayed in Figure 3. Similar to the WT, all mutant peptides analyzed in this work show little change in their near-UV CD in the broad range of temperatures (5−95 °C), solvent conditions (0−1.4 M Gdn HCl or TMAO), or protein concentrations used (0.07−1 mg/mL). Consequently, changes in the secondary (5−75% α-helix) and/or quaternary structure (monomer−oligomer) that occur under these conditions do

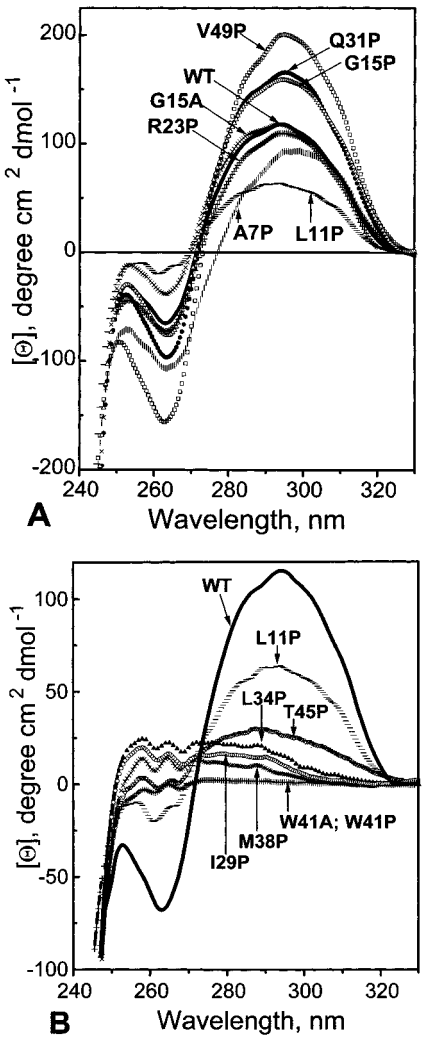

FIGURE 3: Near-UV CD spectra of Pro-containing apoC-1 mutants. Experimental conditions are same as in Figure 2. (A) Near-UV CD similar to that of the WT (—): A7P (|||), L11P (≡), G15P (△), R23P (+), Q31P (●), V49P (□). Spectrum of G15A (×) is given for comparison. (B) Near-UV CD different from that of the WT (—): L11P (≡), I29P (○), L34P (▲), M38P (×), W41P (+), T45P (▽).

not significantly alter the environment of the aromatic groups that contribute to the near-UV CD in these peptides.

Near-UV CD spectra of the mutants can be classified according to their shape as those resembling the spectrum of the WT (Figure 3A) and those substantially differing from it (Figure 3B). The former group includes A7P, G15P, R23P, Q31P, V49P, and L11P that has near-UV CD midway between the two groups. Similar to the WT near-UV CD, these spectra are dominated by a positive peak centered at 295 nm with a shoulder at ∼285 nm, and a smaller negative peak at ∼263 nm (Figure 3A). Variations in the intensity of the mutant spectra, with L11P showing nearly 2-fold reduction and V49P showing almost 2-fold increase in the peak amplitude as compared to the WT, may reflect the effects of mutations on the flexibility of the aromatic cluster that may be propagated via the modulations of the conformational ensemble (*37*). Variations in the near-UV CD intensity may also, in part, result from the differences in the background of the near-UV bands caused by changes in the far-UV region of the mutant spectra. The increased rotational strength of V49P mutant facilitated near-UV CD measure-

ments from V49P solutions of only 0.03 mg/mL concentrations; at these concentrations, apoC-1 should be partially monomeric (*15*). No changes in the molar ellipticity were detected at these peptide concentrations, confirming the absence of any significant contribution from the quaternary packing to the near-UV CD. Furthermore, the spectra in Figure 3A show no correlation between the near-UV CD amplitude and the peptide α-helical content. Thus, G15P has reduced α-helical content of ∼20% (*29*) and Q31P has a slightly increased α-helical content of ∼36% as indicated by far-UV CD (Figure 1), yet their near-UV CD spectra largely superimpose (Figure 3A). Furthermore, R23P has no stable helical structure and G15A has an increased helical content of 45% (*29*), yet their near-UV CD spectra overlap that of the WT (Figure 3A). Observation of nativelike near-UV CD of the R23P mutant, along with the near-native near-UV CD of the thermally or chemically unfolded WT (Figure 2), indicates strongly that the near-UV CD of apoC-1 results from the hydrophobic clustering that persists in the unfolded state rather than from tertiary or quaternary interhelical interactions in the folded state.

Near-UV CD spectra of mutant apoC-1 that substantially differ from the spectrum of the WT, such as I29P, L34P, M38P, W41P, T45P, along with the "midway" spectrum of L11P, are shown in Figure 3B. The spectra of these mutants show large reduction in intensity and large changes in shape as compared to the spectrum of the WT. In I29P, L34P, M38P, and T45P, the amplitude of the positive peak corresponding to ^1L_b transition of Trp is diminished 4−10-fold, suggesting an increased flexibility of W41 side chain. Furthermore, Phe bands at 255−270 nm become positive and reveal fine vibronic structure, with maxima at 258 and 265 nm and minima at 261.5 and 268 nm; similar vibronic bands corresponding to ^1L_b transition of Phe (*35*, *36*) are observed in the spectra of W41P and W41A peptides that lack Trp (Figure 3B). Large Pro-induced spectral changes (Figure 3B) support the notion that the near-UV CD of WT results mainly from the packing of the aromatic groups rather than from their intrinsic ellipticity. Importantly, the spectra in Figure 3A,B show that Pro substitutions causing largest changes in the near-UV CD are located in or near the hydrophobic cluster containing single Trp (W41) and two out of three Phe (F42, F46) in apoC-1 (see Discussion, Figures 5 and 6), suggesting the predominantly local character of this hydrophobic cluster.

CD Measurements of W41A apoC-1. To probe the role of Trp41 side chain in the apoC-1 structure and stability, we recorded far-UV CD data of W41A mutant (Figure 4). The spectrum of W41A (Figure 4, solid line) suggests an extensively unfolded conformation (∼5% α-helix, ∼90% random coil). This spectrum is invariant at 5−90 °C, as indicated by the difference spectrum between the far-UV CD data recorded at 20 and 80 °C (upper inset) and by the temperature invariant ellipticity $[\Theta_{203}](T) \sim -9500$ deg cm^2 dmol^{-1} and $[\Theta_{222}](T) \sim -3500$ deg cm^2 dmol^{-1} at 5−90 °C (lower insert) that is consistent with the random coil conformation. Thus, despite high intrinsic α-helical propensity of Ala as compared to Trp and other amino acids (*38* and references therein), Trp41 to Ala substitution in apoC-1 leads to a complete helical unfolding. Consequently, Trp41 side chain packing is essential for the structural stability of lipid-free apoC-1 in solution.

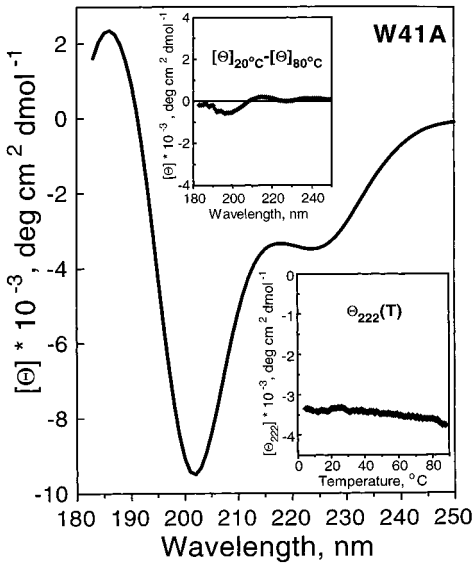

FIGURE 4: Far-UV CD of W41A apoC-1. Spectrum recorded at 20 °C under conditions specified in Figure 1 is shown. Upper inset: Difference spectrum $[\Theta]_{20°C}$ - $[\Theta]_{80°C}$ between the data recorded from the same sample at 20 and 80 °C. Lower inset: Ellipticity $[\Theta_{222}](T)$ recorded upon heating from 5 to 90 °C.

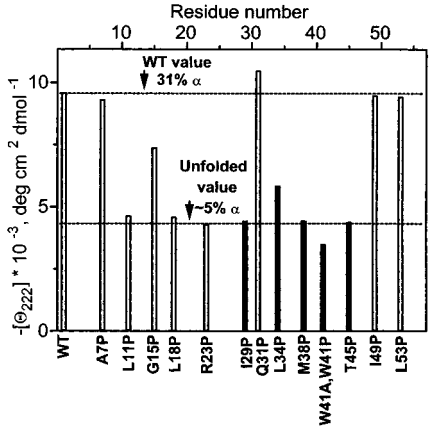

FIGURE 5: Proline scanning mutagenesis of apoC-1: Summary of far- and near-UV CD data. Sites of single Pro substitutions in the apoC-1 sequence are shown along *X*-axis. Bars show the effects of Pro substitutions on the α-helical content as measured by ellipticity at 222 nm; bar filling indicates mutants that have near-UV CD similar to that of the WT (open) or substantially different from it (solid). Dashed horizontal lines show $[\Theta_{222}]$ values of the WT monomer in solution (corresponding to 31% α-helix) and of the chemically or thermally unfolded apoC-1 (∼5% α-helix).

DISCUSSION

Structure of apoC-1 Inferred from Pro Scanning. The results of far- and near-UV CD analysis of apoC-1 mutants are summarized in Figure 5. Far-UV CD results show that Pro substitutions at closely spaced sites separated by only 1−2 groups may have remarkably different effects on the peptide conformation. Thus, I29P leads to a complete unfolding, Q31P causes no unfolding or destabilization, and L34P leads to an apparently incomplete folding of the helical structure (Figures 1 and 5). This suggests that Pro mutagenesis may provide a tool for the secondary structural assignment to apoC-1 and, possibly, other small proteins, with the potential accuracy in selected regions approaching 2 groups. Our assignment was based upon assumption that Pro substitutions leading to complete apoC-1 unfolding are

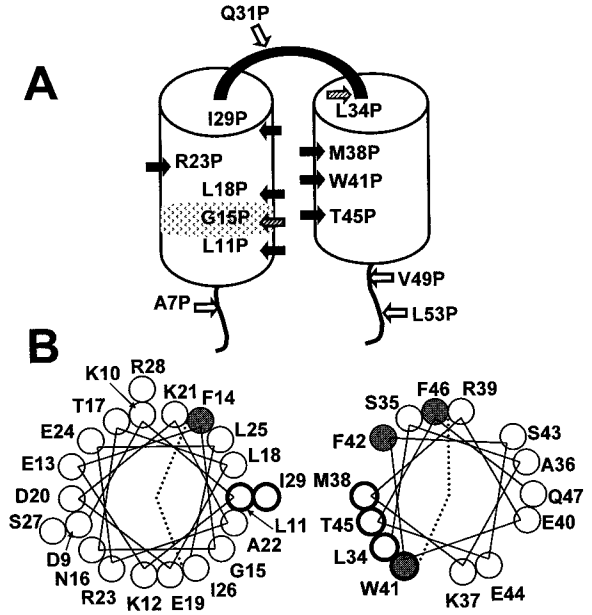

FIGURE 6: Conformation of lipid-free apoC-1 monomer inferred from Pro scanning. (A) Model structure of apoC-1 molecule in solution. The α-helices are shown in cylinders, loop/turn or disordered regions are shown by solid curves, dotted area encompassing G15 shows a kinked/flexible helical region. Arrows indicate Pro substitutions leading to complete unfolding (black), partial unfolding (dashed), or no unfolding (open). (B) Helical wheel representation of the apoC-1 α-helices. Aromatic residues are shown in filled circles. Sites of Pro substitutions leading to large changes in near-UV CD are in bold circles. Apolar helical faces are indicated by dotted lines.

located in the helical regions, those leading to partial unfolding are located in the kinked/flexible regions or peripheral to the helical structure, and those leading to no large unfolding/destabilization are located in disordered/loop regions, in N-cap of an α-helix, or in position 2 of a β-turn where Pro is well tolerated. This simplified assumptions are adequate for a small polypeptide such as apoC-1 that has high helical propensity and lacks extensive tertiary structure, but may have limited applicability to more complex protein systems. The results of our assignment are presented in the model structure of apoC-1 monomer in solution (Figure 6) and are tested by comparison with the predicted and/or observed secondary structures of apoC-1 in lipid-bound and lipid-free states.

The model structure in Figure 6A comprises two helices connected by a short linker containing groups 30−33. This model agrees with the predicted secondary structure of apoC-1 that comprises two α-helices 7−32 and 33−53 separated by a break at 32/33 junction. This break, that was predicted based on the discontinuity in the apolar helical face (*17*), is located in the middle of the interhelical linker in our model, and thus is in excellent agreement with this model.

The model in Figure 6A can be compared with the NMR structure of apoC-1 on SDS micelles (*20*). The observed NMR structures comprise two helices separated by a flexible linker that fall in two groups: a "closed" conformation with interhelical distances <5 Å, and an "open" V-shaped conformation; only the "open" conformation has been reported in detail. Comparison of this "open" conformation with our model shows that the N-terminal helix that spans residues 7−29 in the NMR structure is in excellent agreement with its position inferred from Pro scanning (Figure 6). Furthermore, a helical bend at K12/E13 and high mobility of residues 12−15 detected by NMR is consistent with the flexible and/or kinked helical conformation near G15 inferred from the partial unfolding of G15P mutant (*29*). The C-terminal helix in the NMR structure spans the residues 38−52; in our model, this helix has comparable length but is shifted by about four residues toward the N-terminus, thereby shortening the interhelical linker from eight to about four groups. This difference may be significant and may relate to the structural adaptability of apoC-1. The longer eight-residue linker that is unordered in the NMR structure may facilitate the switching between the "open" and "closed" conformations on SDS micelles, whereas a short ~four-residue linker that likely forms a tight turn may fix the relative orientation of the two helices, thereby facilitating interhelical interactions that stabilize the solution structure of apoC-1.

The helical structure in lipid-free apoC-1 inferred from Pro scanning comprises the total of 36 ± 5 residues, or ~63 ± 9% of the amino acids (Figure 6). This is comparable to the α-helical content in apoC-1 on SDS micelles estimated to be 61% by NMR and 54% by CD (*20*), but is about twice as much as the average helical content estimated by far-UV CD for lipid-free apoC-1 monomer in solution (31 ± 4% α-helix, 60 ± 5% random coil (*29*)). If this latter estimate represented the static protein conformation, Pro substitutions in the unordered regions (i.e., at ~60% of sites) would have caused no helical unfolding and could have even led to entropic stabilization by reducing the configurational entropy of the unfolded state but causing no large changes the enthalpy of the native state or the unfolded state (*27*, *28* and references therein). This is in stark contrast with the observation that the majority of Pro substitutions in apoC-1 are strongly destabilizing (Figure 5), suggesting the dynamic nature of the helical conformation. We therefore propose that the apoC-1 molecule in solution may form fluctuating helical structure that spans a broad range of conformations, from predominantly helical to largely unfolded, leading to an average of 31% helical content observed by far-UV CD. Hence, the increase in the α-helical content of apoC-1 upon lipid binding or self-association may be viewed as a shift in the conformational equilibrium toward the preexisting highly helical conformation rather than de-novo folding of the additional helical segments. Similarly, recent NMR studies of receiver domains, that are the dominant molecular switches in bacterial signaling, revealed a phosphorylation-induced population shift between the preexisting inactive and active conformations, and suggested that stabilization of preexisting protein conformations may be a paradigm for ligand binding (*39*). Our results suggest that apolipoprotein−lipid binding may follow this paradigm.

Interhelical Interactions and Minimal Folding Units. Far-UV CD results summarized in Figures 5 and 6 show that single Pro substitutions at several sites in the N-terminal helix (e.g., L11P, L18P, R23P, I29P) or in the C-terminal helix (e.g., M38P, W41P, T45P) lead to a complete loss of the helical structure in apoC-1. Thus, unfolding one helix by a Pro substitution leads to the unfolding of the second helix. Similarly, deleting one apoC-1 α-helix leads to the unfolding of the second helix, as demonstrated by the spectroscopic studies of A. Rozek et al. (*18*, *19*) showing that apoC-1 fragments 1−38 (containing 11-mer sequence repeats I−III)

and 35−53 (containing part of repeat II and repeat III) that encompass individual α-helices are unstructured in solution. These results point to the importance of the interhelical interactions for the stability of the lipid-free apoC-1 (*29*) and suggest that the minimal folding unit in apoC-1 comprises two helices formed of four 11-mer sequence repeats, folded in a helix−turn−helix motif and stabilized by interhelical interactions (Figure 6A).

ApoC-1 is the smallest human apolipoprotein thought to be closely related to the primordial gene from which larger apolipoproteins have evolved via duplication and/or deletion of 11-mer codon repeats (*40*). Class-A amphipathic α-helices in apoC-1 are highly homologous to those in larger apolipoproteins and have similar proportions of the apolar surface area (∼40% in apoC-1, 30−50% in other exchangeable apolipoproteins) (*16*). This suggests that the minimal folding unit in apoC-1 may be similar to that in larger apolipoproteins. Indeed, similar to apoC-1, apoA-1 fragment 99−142, that comprises two 22-mer repeats predicted to form two class-A amphipathic α-helices connected by a turn, is ∼30% helical in solution (Yang Chao, Ph.D. Thesis, Boston University School of Medicine, in preparation). We, therefore, propose that the minimal folding unit in larger apolipoproteins in solution may also be a helix−turn−helix motif comprised of four 11-mer, or two 22-mer, sequence repeats. Analysis of other α-helical repeat proteins, such as armadillo-related proteins or ankyrin repeat proteins, led to the hypothesis that all such proteins require multiple repeat units to stabilize their structure (*41*, and references therein). Our analysis corroborates this hypothesis and suggests that apolipoproteins may represent another family of helical repeat proteins with minimal folding modules formed of at least two repeat motifs.

In contrast to apoC-1 that has no prolines in its 11-mer sequence repeats, larger apolipoproteins such as apoA-1 or apoE are comprised of 22-mer repeats containing Pro in position 1 of the repeat. The suggested role of Pro punctuation is in introducing a kink or terminating individual helices, thereby optimizing lipid−protein interactions on the curved lipoprotein surfaces (*16*, *17*). We suggest that Pro punctuation may also optimize the formation of the interhelical turn regions, thereby facilitating the folding of the autonomous helix−turn−helix modules in lipid-free apolipoproteins.

Near-UV CD and Residual Aromatic Clustering. Protein near-UV CD spectra arise from the asymmetry in the environment of the aromatic groups that usually results from the tertiary packing; several proteins have also been reported to have significant contributions from quaternary packing to their near-UV CD (*42*−*44*). Our results suggest that apoC-1 is an exception to this rule. Indeed, the normalized near-UV CD of the WT apoC-1 remain invariant upon decreasing the protein concentration from 1 to 0.07 mg/mL (0.03 mg/mL for V49P) or increasing Gdn HCl concentration from 0 to 1.4 M, thereby substantially reducing or even eliminating (in the presence of Gdn HCl) protein self-association. Consequently, quaternary interactions do not significantly contribute to the near-UV CD of apoC-1. Furthermore, correlation of far- and near-UV CD recorded of WT apoC-1 in a broad range of temperatures and solvent conditions shows that large changes in the α-helical content, from ∼5% (at 80 °C or in 1.4 M Gdn HCl) to ∼75% (in 1 M TMAO), are not accompanied by any large changes in the near-UV CD (Figure 2). Similarly, loss of the α-helical structure induced by mutations such as R23P may not be accompanied by any significant changes in the near-UV CD (Figure 3A). In addition, similar to the wild-type apoC-1, near-UV CD spectra of all mutant peptides analyzed in our study persist at high temperatures (up to 90 °C) or in high Gdn HCl concentrations (1.4 M), i.e., under conditions where the helical structure is unfolded. Taken together, these results indicate strongly that the dominant contribution to the near-UV CD of apoC-1 comes from the clustering of aromatic groups that persists in the unfolded state rather than from the tertiary or quaternary helical packing in the folded state.

To our knowledge, there is but one report of the near-UV CD observed in the Gdn HCl unfolded (but not in the heat unfolded) state of WW domain, a β-sheet protein module that mediates protein−protein interactions (*45*). Our results extend this observation to thermal, chemical, and Pro-unfolded states of an α-helical protein. In contrast to non-native near-UV CD of the chemically unfolded WW domain, near-UV CD spectra of the apoC-1 peptides recorded in the folded and in the unfolded states are similar. Consequently, the aromatic cluster encompassing W41, F42, and F46, which is the major contributor to the near-UV CD of the unfolded apoC-1, is compatible with the helical conformation. Therefore, this cluster is likely to form the most stable helical element and may serve as a template for the helical folding in other apoC-1 regions. The importance of local interactions for the packing of this aromatic cluster is suggested by the observation that Pro substitutions leading to largest near-UV CD changes (Figure 3B) are located in the vicinity of this cluster: L34, M38, and T45, together with W41, F42, and F46 form continuous apolar face of the C-helix, and I29 from the adjacent apolar face of the N-helix is juxtaposed to L34 and may interact with it (Figure 6). Nonlocal interactions may also be important, as suggested by substantial near-UV CD changes induced by L11P substitution (Figures 3 and 6). Similar hydrophobic clusters forming nativelike structure stabilized by local and nonlocal interactions have been detected by NMR and other physicochemical techniques in the unfolded states of several globular proteins (*46*−*50* and references therein) and have been proposed to nucleate the folding of some of these proteins (*46*, *48*). In apoC-1, the aromatic cluster encompassing W41 may not only be involved in the helix nucleation but is also essential for the stability of the lipid-free conformation, as indicated by the complete loss of the helical structure in W41A mutant (Figure 4).

Aromatic residues have been proposed to play a dominant role in anchoring apolipoproteins to lipid surfaces (*51*). Furthermore, the tendency of aromatic residues to cluster with a concomitant bend in the helix observed in the NMR structures of apoC-1 (*20*) and of apoE fragment on SDS (*51*) was proposed to enhance the binding of amphipathic α-helices to the curved lipoprotein surfaces (*20*). Our results indicate that aromatic groups, such as W41 in apoC-1, may also be essential for the stability of the lipid-free apolipoprotein conformation, and suggest that hydrophobic clusters containing aromatic groups may form the most stable helical elements in apolipoproteins.

ACKNOWLEDGMENT

Author is grateful to Dr. David Atkinson for many useful discussions and for the critical reading of the manuscript prior to publication, and to Ranjana for help with the manuscript preparation.

REFERENCES

1. Mahley, R. W., Innerarity, T. L., Rall, S. C., and Weisgraber, K. H. (1984) *J. Lipid Res. 25(12)*, 1277−1294.
2. Atkinson, D., and Small, D. M. (1986) *Annu. Rev. Biophys. Biophys. Chem. 15*, 403−456.
3. Eisenberg, S. (1990) *Curr. Opin. Lipidol. 1*, 205−215.
4. Glomset, J. A., Janssen, E. T., Kennedy, R., and Dobbins, J. (1966) *J. Lipid Res. 7*, 638−648.
5. Windler, E., and Havel, R. J. (1985) *J. Lipid Res. 26*, 556−565.
6. Steyrer, E., and Kostner, G. M. (1988) *Biochim. Biophys. Acta 958*, 484−491.
7. Gautier, T., Masson, D., de Barros, J. P., Athias, A., Gambert, P., Aunis D., Metz-Boutigue, M. H., and Lagrost, L. (2000) *J. Biol. Chem. 275(48)*, 37504−37509.
8. Kinnunen, P. C., and Enholm, C. (1976) *FEBS Lett. 65*, 354−357.
9. Poensgen, J. (1990) *Biochim. Biophys. Acta 1042(2)*, 188−192.
10. Tournier, J. F., Bayard, F., and Tauber, J. P. (1984) *Biochim. Biophys. Acta 804(2)*, 216−220.
11. Swaney, J. B., and Weisgraber, K. H. (1994) *J. Lipid Res. 35(1)*, 134−142.
12. Weisgraber, K. H., Mahley, R. W., Kowal, R. W., Herz, J., Goldstein, J. L., and Brown, M. S. (1990) *J. Biol. Chem. 265*, 22453−22459.
13. Sehayek, E., and Eisenberg, S. (1991) *J. Biol. Chem. 266*, 18259−18267.
14. Nestel, P. J., and Fidge, N. H. (1982) *Adv. Lipid Res. 19*, 55−83.
15. Osborne, J. C., Jr., Bronzert, T. J., and Brewer, H. B., Jr. (1977) *J. Biol. Chem. 252*, 5756−5760.
16. Segrest, J. P., De Loof, H., Dohlman, J. G., Brouillette, C. G., and Anantharamaiah, G. M. (1990) *Proteins 8*, 103−117.
17. Segrest, J. P., Jones, M. K., De Loof, H., Brouillette, C. G., Venkatachalapathi, Y. V., and Anantharamaiah, G. M. (1992) *J. Lipid Res. 33*, 141−166.
18. Rozek, A., Buchko, G. W., and Cushley, R. J. (1995) *Biochemistry 34*, 7401−7408.
19. Rozek, A., Buchko, G. W., Kanda, P., and Cushley, R. J. (1997) *Protein Sci. 6*, 1858−1868.
20. Rozek, A., Sparrow, J. T., Weisgraber, K. H., and Cushley, R. J. (1999) *Biochemistry 38(44)*, 14475−14484.
21. Gursky, O., and Atkinson, D. (1996) *Proc. Natl. Acad. Sci. U.S.A. 93*, 2991−2995.
22. Gursky, O., and Atkinson, D. (1998) *Biochemistry 37*, 1283−1291.
23. Osborne, J. C., Jr., Lee, N. S., and Powell, G. M. (1986). Solution properties of apolipoproteins. *Methods Enzymol. 128*, 375−387.
24. Lu, B., Morrow, J. A., and Weisgraber, K. H. (2000) *J Biol. Chem. 275(27)*, 20775−20781.
25. Segelke, B. W., Forstner, M., Knapp, M., Trakhanov, S. D., Parkin, S., Newhouse, Y. M., Bellamy, H. D., Weisgraber, K. H., and Rupp, B. (2000) *Protein Sci. 9(5)*, 886−897.
26. Schulman, B. A., and Kim, P. S. (1996) *Nat. Struct. Biol. 3*, 682−687.
27. Shortle, D. (1989) *J. Biol. Chem. 264*, 5315−5318.
28. Sturtevant, J. M. (1993) *Pure Appl. Chem. 65*, 991−998.
29. Gursky, O. (1999) *Protein Sci. 8*, 2055−2064.
30. Sigler, G. F., Soutar, A. K., Smith, L. C., Gotto A. M., Jr., and Sparrow, J. T. (1976) *Proc. Natl. Acad. Sci. U.S.A. 73*, 1422−1426.
31. Harding, D. R., Batter, J. E., Husbands, D. R., and Hancock, W. S. (1976) *J. Am. Chem. Soc. 98*, 2644−2645.
32. Mao, D. and Wallace, B. A. (1984) *Biochemistry 23*, 2667−2673.
33. Venyaminov, S. Y. and Vassilenko, K. S. (1994) *Anal. Biochem. 222*, 176−184.
34. John, D. M., and Weeks, K. M. (2000) *Protein Sci. 9*, 1416−1419.
35. Stickland, E. H. (1974) *Crit. Rev. Biochem. 2*, 113−175.
36. Woody, R. W. and Dunker, A. K. (1996) in *Circular Dichroism and Conformational Analysis of Biomolecules* (Fasman, G. D., Edt.) pp 110−157, Plenum Press, New York.
37. Pan, H., Lee, J. C., and Hilser, V. (2000) *Proc. Natl. Acad. Sci. U.S.A. 97(22)*, 12020−12025.
38. Kallenbach, N. R., Lyu, P., and Zhou, H. (1996) *Circular Dichroism and Conformational Analysis of Biomolecules* (Fasman, G. D., Ed.) Plenum Press NY, pp 201−260.
39. Kern D., Volkman, B. F., and Wemmer, D. E. (2001) *Biophys. J. 80(1/2)*: 13a.
40. Luo, C. C., Li, W. H., Moore, M. N., and Chan, L. (1986). *J. Mol. Biol. 187(3)*, 325−340.
41. Zhang, B., and Peng, Z-y. (2000) *J. Mol. Biol. 299(4)*, 1121−1132.
42. Li, R., Nagai, Y., and Nagai, M. (2000) *J. Inorg. Biochem. 82(1−4)*, 93−101.
43. Liang, J. J., and Chakrabarti, B. (1998) *Biochem. Biophys. Res. Commun. 246(2)*, 441−445.
44. Colon, W., and Kelly, J. W. (1992) *Biochemistry 31(36)*, 8654−8660.
45. Koepf, E. K., Petrassi, H. M., Sudol, M., and Kelly, J. W. (1999) *Protein Sci. 8(4)*, 841−853.
46. Neri, D., Billeter, M., Wider, G., and Wuthrich, K. (1992) *Science 257*, 1559−1563.
47. Logan, T. M., Theriault, Y., and Fesik, S. W. (1994) *J. Mol. Biol. 236(2)*, 637−648.
48. Arcus, V. L., Vuilleumier, S. Freund, S. M., Bycroft, M., and Fersht, A. R. (1995) *J. Mol. Biol. 254(2)*, 305−321.
49. Saab-Rincon, G., Gualfetti, P. J., and Matthews, C. R. (1996) *Biochemistry 35(6)*, 1988−1994.
50. Hackel, M., Konno, T., and Hinz, H. (2000) *Biochim. Biophys. Acta 1479(1−2)*, 155−165.
51. Wang, G., Pierens, G. K., Treleaven, W. D., Sparrow, J. T., and Cushley, R. J. (1996) *Biochemistry 35(32)*, 10358−10366.

BI0111505